

Quantum Phase Transition in a Quantum Ising Chain at Nonzero Temperatures

K. L. Zhang and Z. Song*

School of Physics, Nankai University, Tianjin 300071, China

We study the response of a thermal state of an Ising chain to a nonlocal non-Hermitian perturbation, which coalesces the topological Kramer-like degeneracy in the ferromagnetic phase. The dynamic responses for initial thermal states in different quantum phases are distinct. The final state always approaches its half component with a fixed parity in the ferromagnetic phase but remains almost unchanged in the paramagnetic phase. This indicates that the phase diagram at zero temperature is completely preserved at finite temperatures. Numerical simulations for Loschmidt echoes demonstrate such dynamical behaviors in finite-size systems. In addition, it provides a clear manifestation of the bulk-boundary correspondence at nonzero temperatures. This work presents an alternative approach to understanding the quantum phase transitions of quantum spin systems at nonzero temperatures.

Introduction.—A conventional quantum phase transition (QPT) [1] describes an abrupt change in matter at zero temperature. At nonzero temperatures, the existence of quantum critical behavior depends on the competition between thermal and quantum fluctuations. At higher temperatures, thermal fluctuations conceal the quantum criticality, thus leaving no residuals of quantum phase diagram at absolute zero temperature. On the other hand, variations in a parameter across the critical point induces a symmetry spontaneous breaking of the ground state. The underlying mechanism is the degeneracy of the ground states. These features have been demonstrated in a one-dimensional (1D) quantum Ising model with a transverse field, which is exactly solvable, so as to be a unique paradigm for understanding conventional QPTs. In recent works [2, 3], it turns out that the local order parameter and topological index can coexist to characterize the QPT.

In this Letter, we revisit the Ising model to investigate the existence of QPT at nonzero temperatures—a seldom discussed topic. It is motivated from the duality of the Kitaev model, which describes 1-D spinless fermions with superconducting p -wave pairing [4]. The Kitaev model is the fermionized version of the familiar 1-D transverse-field Ising model [5], an easily solvable model exhibiting quantum criticality and QPT with spontaneous symmetry breaking [1]. Also, as the gene of a Kitaev model, the Majorana lattice is the Su-Schrieffer-Heeger (SSH) model [6], which has served as a paradigmatic example of a 1-D system supporting topological characteristic [7]. It manifests the key features of topological order because the number of zero-energy levels and edge states are immune to local perturbations [8].

At nonzero temperatures, there are various approaches to study quench dynamics of the Ising model and the XXZ model, for example, the form factor expansions [9, 10] and the quantum transfer matrix approaches [11, 12]. A typical method for detecting QPT is to monitor the response of the ground state under a perturbation through the implementation of Loschmidt echo (LE) and fidelity [13–19]. Most perturbations applied to the

Ising model are Hermitian terms, the simplest example of which is the shift of the transverse field. Nevertheless, since the discovery that a class of non-Hermitian Hamiltonians could exhibit entirely real spectra [20–23], the non-Hermitian Hamiltonian is no longer a forbidden regime in quantum mechanics. A certain type of non-Hermitian term may have exclusive effects never before observed in a Hermitian system [24–27]. More importantly, natural quantum systems such as cold atom systems are intrinsically non-Hermitian because of spontaneous decay [28–33]. In this work, we study the response of a thermal state of an Ising chain to a non-Hermitian perturbation, which coalesces the topological Kramer-like degeneracy in the ferromagnetic phase. We use LEs to measure the response and observe that they are distinct for initial thermal states in different quantum phases. The exceptional point (EP) drives a thermal state approaching to its half component in the ferromagnetic phase but remain unchanged in the paramagnetic phase. Numerical simulations for LE demonstrate such dynamical behaviors in finite-size systems. In addition, it presents a clear manifestation of the bulk-boundary correspondence at nonzero temperature. The underlying mechanism is that within the ferromagnetic phase, the robust degeneracy occurs not only in the ground states, but in all energy levels, allowing the identification of the nature of quantum phases from a thermal state. It indicates that the phase diagram at zero temperature is completely preserved at finite temperatures [see Fig. 1(a)], comparing to the phase diagram [see Fig. 1(b)] studied in terms of correlation function in the work of Sachdev *et al.* [1, 34]. This property promises the stable ground states, and enables theoretical and experimental investigations of QPT through dynamical control and testing. We present an alternative approach for understanding the QPT of quantum spin systems at nonzero temperatures.

Model and degenerate spectrum.—The model considered is the transverse field Ising chain with open bound-

ary condition, defined by the Hamiltonian

$$H = -J \sum_{j=1}^{N-1} \sigma_j^x \sigma_{j+1}^x + g \sum_{j=1}^N \sigma_j^z, \quad (1)$$

where σ_j^α ($\alpha = x, y, z$) are the Pauli operators on site j and parameter g ($g \geq 0$) is the transverse field strength. For simplicity, the following discussion assumes that $J = 1$. We first review some well-known model properties that are crucial to our conclusion. The parity $p = \prod_{j=1}^N (-\sigma_j^z)$ is determined to be conservative; that is, $[p, H] = 0$ is always true.

The model with periodic boundary condition is exactly solvable and has been well studied [5]. At zero temperature, QPT at $g = 1$ separates a ferromagnetic phase of the system ($g < 1$) from a paramagnetic phase ($g > 1$). In general, model properties are not sensitive to the boundary condition in thermodynamic limit. However, herein we consider the model with open boundary condition, which notably possesses an exclusive symmetry in the ferromagnetic phase $g < 1$, and it is also the key point of this work. It can be checked that in thermodynamic limit, we have a nonlocal operator [35]

$$D = \frac{1}{2} \sqrt{1 - g^2} \sum_{j=1}^N g^{j-1} D_j, \quad (2)$$

with a position-dependent component

$$D_j = \prod_{l < j} (-\sigma_l^z) \sigma_j^x - i \prod_{l < N-j+1} (-\sigma_l^z) \sigma_{N-j+1}^y, \quad (3)$$

(where $i = \sqrt{-1}$), satisfying the commutation relations

$$[D, H] = [D^\dagger, H] = 0, \quad (4)$$

that can be regarded as a symmetry of the system. In addition, the relations $\{D, D^\dagger\} = 1$ and $D^2 = (D^\dagger)^2 = 0$ [35] suggest that D is a fermion operator, which can be related to the edge operator of the Kitaev chain [4] $D \rightarrow \frac{1}{2} \sqrt{1 - g^2} \sum_{j=1}^N [(g^{j-1} + g^{N-j}) c_j^\dagger + (g^{j-1} - g^{N-j}) c_j]$ (where c_j is a fermion operator) by the Jordan-Wigner transformation [36]. Importantly, such a symmetry is a little special, because it is contingent on the following conditions: $g < 1$, a large N limit, and open boundary. Particularly, operator D is nonuniversal and Hamiltonian dependent because it contains the parameter g from the Hamiltonian. The first two conditions accord with the symmetry breaking mechanism of QPT [1]. Actually, the commutation relations in Eq. (4) guarantee the existence of eigenstate degeneracy. Specifically, there is a set of degenerate eigenstates $\{|\psi_n^+\rangle, |\psi_n^-\rangle\}$ of H with eigenenergy E_n , in two invariant subspaces, i.e., $H|\psi_n^\pm\rangle = E_n|\psi_n^\pm\rangle$ and $p|\psi_n^\pm\rangle = \pm|\psi_n^\pm\rangle$. Figure 1(c) presents the spectrum of the low-lying states, which possess distinct degenerate structures in two phases. Furthermore, we have the

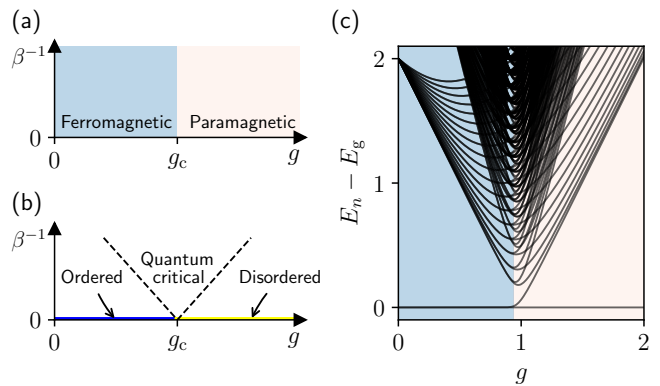


FIG. 1. (a) Phase diagram detected from the LEs in this work. (b) Phase diagram studied in term of correlation function in the work of Sachdev *et al.*. Here β^{-1} is the temperature and g_c is the quantum critical point. (c) Spectrum of the low-lying states for a finite quantum Ising chain as a function of g , obtained numerically through exact diagonalization. E_g is the ground-state energy. System parameters: $N = 50$ and $J = 1$. The energy gap closes at a quasicritical point, indicated by the boundary of the two shaded areas. Notably, all energy levels become twofold degeneracy simultaneously at one point, protected by the symmetry of the quasi-zero-mode operator D .

relations

$$D|\psi_n^+\rangle = |\psi_n^-\rangle, D^\dagger|\psi_n^-\rangle = |\psi_n^+\rangle, D^\dagger|\psi_n^+\rangle = D|\psi_n^-\rangle = 0, \quad (5)$$

in the ferromagnetic phase. We refer to this property as topological Kramers-like degeneracy for two reasons: (i) the twofold degeneracy lies in the full spectrum, and (ii) it is invariant in the presence of random, position-dependent deviation on the field g , where a new operator D is redefined accordingly [35]. Because of this property, operator D plays an important role in the quench dynamics, as demonstrated in the following section.

Non-Hermitian perturbation and EP dynamics.—In general, a Hermitian perturbation can lift the degeneracy. However, a non-Hermitian perturbation may take a surprising effect. A fascinating phenomenon is the coalescence of two degenerate states, which supports exclusive dynamics never occurs in a Hermitian system. Such degeneracy-related dynamics differentiates the quantum phases at any temperature, not only in the ground states. To this end, we introduce operator D into the post-quench Hamiltonian \mathcal{H} by treating it as a perturbation

$$\mathcal{H} = H + \kappa D, \quad (6)$$

with $\kappa \ll g$. For a system in the ferromagnetic phase, where $0 < g < 1$, any pair of degenerate eigenstates ($|\psi_n^+\rangle, |\psi_n^-\rangle$) with energy E_n spans a diagonal block with the sub-Hamiltonian

$$\mathcal{H}_n = \begin{pmatrix} E_n & 0 \\ \kappa & E_n \end{pmatrix}, \quad (7)$$

which has a Jordan block structure. This means that in the ferromagnetic phase, the degenerate spectrum becomes an exceptional spectrum with a set of coalescing states $\{|\psi_n^c\rangle\} = \{|\psi_n^-\rangle\}$ when the non-Hermitian term κD is introduced. The diagonal Jordan block is exact for any values of κ . By contrast, for a system in the paramagnetic phase, κD does not considerably affect the energy levels of H when g is much larger than 1 ($H \approx g \sum_{j=1}^N \sigma_j^z$ in this case); this is because the gap between energy levels with different parities is at least in the order of g [see Fig. 1(c)].

On the basis of this analysis, the dynamics in the ferromagnetic phase is governed by the time evolution operator

$$U(t) = \exp(-i\mathcal{H}t) = \prod_n U_n(t), \quad (8)$$

where the time evolution operator in the n th subspace has the form $U_n(t) = \exp(-i\mathcal{H}_n t) = \exp(-iE_n t) [1 - i(\mathcal{H}_n - E_n)t]$ based on the identity $(\mathcal{H}_n - E_n)^2 = 0$ for $g < 1$. The dynamics of a pure initial state are then clarified, as given in $U_n(t)(a|\psi_n^-\rangle + b|\psi_n^+\rangle) = \exp(-iE_n t)[(a - itb\kappa)|\psi_n^-\rangle + b|\psi_n^+\rangle]$. The action of $U_n(t)$ over a long period projects any pure initial state on the component $|\psi_n^-\rangle$, which is completely different from that in the paramagnetic phase. These features allow us to observe significantly different dynamical behaviors for a initial thermal state.

QPT at nonzero temperatures.—We have observed that the difference between spectra in two regions not only lies in the ground states but also the full spectrum. This results in the exclusive EP dynamics for the initial state involving any excited eigenstates in the ferromagnetic phase, from which two phases at finite temperatures can be identified. Notably, bulk-boundary correspondence can manifest at nonzero temperatures. In the following, we focus on the dynamics of a initial thermal state with density matrix $\rho(0) = e^{-\beta H} / \text{Tr} e^{-\beta H}$ at temperature β for a system (pre-quench Hamiltonian) H under a quenched non-Hermitian Hamiltonian $\mathcal{H} = H + \kappa H'$ where H' is non-Hermitian, and κ is real.

As mentioned, operator D is g dependent, and a matching D in the perturbation leads to an exact EP. Nevertheless, operator D_j (or D_j^\dagger) still takes the role to switch the parity of an eigenstate and forms a Jordan block approximately for a sufficiently small κ . Operators D and D_j ($j \in [1, N]$) are nonlocal combinations of spin operators $\{\sigma_j^x\}$ and $\{\sigma_j^y\}$ for a quantum spin system, and D_1 is the main component of D . We consider two cases of H' where it is (i) a dominant term of operator D (i.e., $H' = D_1$) and (ii) position dependent (i.e., $H' = D_j$). After the quench, the time evolution of the thermal state obeys the equation

$$i \frac{\partial}{\partial t} \rho(t) = \mathcal{H} \rho(t) - \rho(t) \mathcal{H}^\dagger, \quad (9)$$

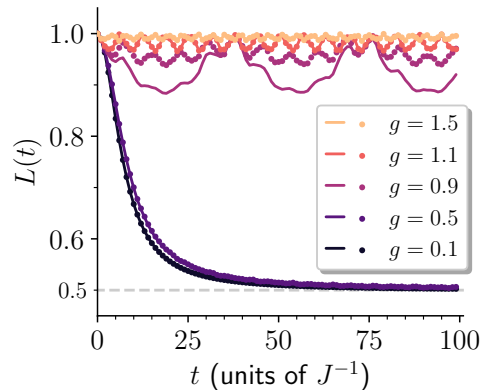


FIG. 2. LEs of different g values. The lines and dots represent the LEs for $\beta = 5$ and $\beta = 10$, respectively. Other parameters: $N = 10$, $\kappa = 0.1$, and $J = 1$. The profiles of the LEs in the two regions are distinct, independent of the temperature of the initial thermal states, and converge to 1.0 and 0.5, respectively.

which admits the formal solution

$$\rho(t) = e^{-i\mathcal{H}t} \rho(0) e^{i\mathcal{H}^\dagger t}. \quad (10)$$

Unlike the Hermitian case, the time evolution of the density matrix is no longer unitary. Thus, in the following numerical calculation, we normalize $\rho(t)$ by taking [37, 38]

$$\rho(t) = e^{-i\mathcal{H}t} \rho(0) e^{i\mathcal{H}^\dagger t} / \text{Tr} [e^{-i\mathcal{H}t} \rho(0) e^{i\mathcal{H}^\dagger t}]. \quad (11)$$

To characterize the degree of distinguishability between the initial state $\rho(0)$ and evolved state $\rho(t)$, we introduce the LE

$$L(t) = \left[\text{Tr} \sqrt{\sqrt{\rho(0)} \rho(t) \sqrt{\rho(0)}} \right]^2, \quad (12)$$

also known as the Uhlmann fidelity [39, 40]. The value of $L(t)$ after a sufficient period can be estimated intuitively. In general, an initial mixed state $\rho(0)$ contains components of two parities. In the ferromagnetic phase, the component with a certain parity of the thermal state $\rho(t)$ is dominant because of EP dynamics, and in large t limits, the LE $L(t)$ approaches 0.5. In the paramagnetic phase, a non-Hermitian perturbation does not substantially affect the dynamics; this is expressed by $L(t) \approx L(0) = 1$. We now numerically demonstrate the decay behavior of $L(t)$ within a short period.

First, we consider the quench dynamics under the postquench Hamiltonian $\mathcal{H} = H + \kappa D_1$. We conduct numerical simulations for $L(t)$ for the initial state $\rho(0)$ at different phases in the finite system. The computations are performed using a uniform mesh in the time discretization for the Hamiltonian \mathcal{H} . As mentioned, the spectral degeneracy is dependent on a large N limit.

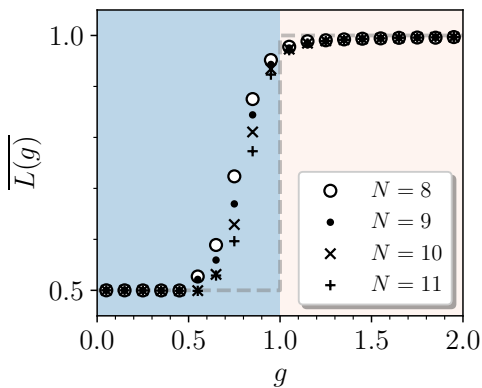


FIG. 3. Average LEs as functions of g when $N = 8, 9, 10$, and 11 . The dashed line represents the ideal average LEs expected for large N limits. Here we set $\tau = 500$ and $T = 500$. Other parameters: $\kappa = 0.1$, $J = 1$, and $\beta = 1$. It indicates that as N increases, the plots have the trends to the prediction in the thermodynamic limit.

However, a sufficiently small g still leads to perfect quasidegeneracy in finite-size systems [35]. Consistent with our prediction, the numerical results of LEs in Fig. 2 are insensitive to temperature and tend towards different values in different phases.

To determine the effect of g , we introduce an average LE in the time interval $[\tau, \tau + T]$, defined as follows:

$$\bar{L} = \frac{1}{T} \int_{\tau}^{\tau+T} L(t) dt, \quad (13)$$

where $\tau \gg 1$. Average LEs as functions of parameter g for different N values are plotted in Fig. 3. When N is larger, the average LE is closer to the ideal values that are expected in the thermodynamic limit. This indicates that the LEs can be used to identify the quantum phase diagram at nonzero temperatures even in small size systems.

Second, we investigate the bulk-boundary correspondence at nonzero temperatures through quench dynamics. Consider the post-quench Hamiltonian with the form

$$\mathcal{H} = H + \kappa D_j, \quad (14)$$

where D_j , defined in Eq. (3), is the component of operator D . In this case, the LE is denoted by $L_j(t)$. The long-term behavior of $L_j(t)$ when $j > 1$ is expected to be similar to $L(t)$ of the postquench Hamiltonian in the first case. We are interested in the dependence of $L_j(t)$ in different phases on position over a short period. The numerical simulation results are plotted in Fig. 4. We can see that, (i) in the case of $g < 1$, $L_j(t)$ tends towards 0.5 for the j near the end and decays more rapidly as j approaches the boundary. By contrast, in the case of $g > 1$, $L_j(t)$ remains at 1.0 for all j . And (ii) in the case of $g = 0.1$, the LEs in the middle do not decay but remain

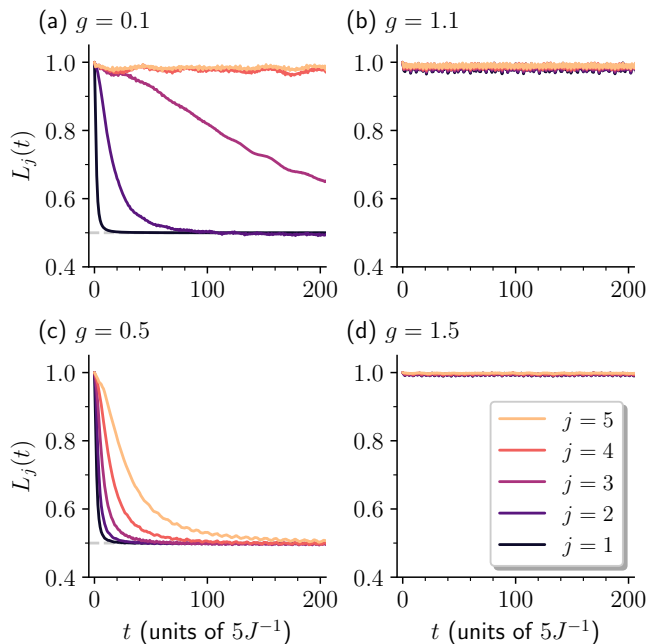


FIG. 4. Simulation results for LEs under the postquench Hamiltonian (14) for different j values. (a) and (c) LEs in the ferromagnetic phase when $g = 0.1$ and 0.5 . (b) and (d) LEs in the paramagnetic phase when $g = 1.1$ and 1.5 . Other parameters: $N = 10$, $J = 1$, $\kappa = 0.1$, and $\beta = 1$. The LE decays rapidly to 0.5 at the end of the chain in the ferromagnetic phase, whereas it remains at one in the paramagnetic phase. In the case (a), where g is small, the LEs in the middle do not decay but remain near 1.0, which implies the LE behavior in long chains. This is a clear manifestation of the bulk-boundary correspondence at nonzero temperatures.

near a value of one. The expression of D indicates that in the ferromagnetic phase $g < 1$, small g values enhances the edge effect compared with the case of large g [41]. This suggests that similar effects can be observed in any case of a sufficiently long chain where $g < 1$. In addition, this demonstrates that $L_j(t)$ defines the bulk-boundary correspondence for Ising chains at nonzero temperatures.

Discussion.— In summary, we extended the quantum phase diagram for Ising chains from zero to nonzero temperatures. The degeneracy spectrum of the system in the ferromagnetic phase, which arises from Majorana zero modes, is the crux of our conclusion. Such nonzero-temperature QPT can be detected through the response of a thermal state to a nonlocal non-Hermitian perturbation on the Ising chain. The non-Hermiticity of the perturbation dynamically amplifies the difference between two quantum phases. The EP dynamics for coalescing states have no counterpart in the Hermitian regime and allow distinct responses for initial thermal states in the two quantum phases. Numerical simulations for LE also provides a clear manifestation of the bulk-boundary correspondence at nonzero temperatures in the quantum

spin system. This is an alternative approach for understanding the QPT of quantum spin systems at nonzero temperatures. The possible experimental implementations to verify our results would be a diamond system [42] and polycrystalline adamantane system [43], where the dynamical behaviors in quantum spin systems at nonzero temperature were observed.

Several points should be addressed before ending this Letter. (i) The nonlocal factor $\prod_{l < j} (-\sigma_l^z)$ in operator D_j has a crucial role in the simulations; when it is omitted, the EP cannot appear again. (ii) In the presence of disordered parameters J and g in the Hamiltonian, the observed results still hold [35]. (iii) The approach based on thermal state fidelity can also be applied to the non-Hermitian model $\mathcal{H}(g) = H + \kappa D$. Any thermal state always has a fixed parity in the ferromagnetic phase, while it has half component with each party in the paramagnetic phase. This leads to a sudden drop in the thermal fidelity at the critical point.

This work was supported by the National Natural Science Foundation of China (under Grant No. 11874225).

* songtc@nankai.edu.cn

- [1] S. Sachdev, *Quantum phase transitions* (1999).
- [2] G. Zhang and Z. Song, Topological characterization of extended quantum ising models, *Phys. Rev. Lett.* **115**, 177204 (2015).
- [3] G. Zhang, C. Li, and Z. Song, Majorana charges, winding numbers and chern numbers in quantum ising models, *Sci. Rep.* **7**, 1 (2017).
- [4] A. Y. Kitaev, Unpaired majorana fermions in quantum wires, *Phys. Usp.* **44**, 131 (2001).
- [5] P. Pfeuty, The one-dimensional ising model with a transverse field, *Ann. Phys.* **57**, 79 (1970).
- [6] W. P. Su, J. R. Schrieffer, and A. J. Heeger, Solitons in polyacetylene, *Phys. Rev. Lett.* **42**, 1698 (1979).
- [7] J. Zak, Berry's phase for energy bands in solids, *Phys. Rev. Lett.* **62**, 2747 (1989).
- [8] J. K. Asbóth, L. Oroszlány, and A. Pályi, *A short course on topological insulators* (Springer, 2016).
- [9] M. Dugave, F. Göhmann, and K. K. Kozłowski, Thermal form factors of the xxz chain and the large-distance asymptotics of its temperature dependent correlation functions, *J. Stat. Mech.* **2013**, P07010 (2013).
- [10] E. Granet, M. Fagotti, and F. H. L. Essler, Finite temperature and quench dynamics in the Transverse Field Ising Model from form factor expansions, *SciPost Phys.* **9**, 33 (2020).
- [11] M. Suzuki, Transfer-matrix method and monte carlo simulation in quantum spin systems, *Phys. Rev. B* **31**, 2957 (1985).
- [12] F. Andraschko and J. Sirker, Dynamical quantum phase transitions and the loschmidt echo: A transfer matrix approach, *Phys. Rev. B* **89**, 125120 (2014).
- [13] H. T. Quan, Z. Song, X. F. Liu, P. Zanardi, and C. P. Sun, Decay of loschmidt echo enhanced by quantum criticality, *Phys. Rev. Lett.* **96**, 140604 (2006).
- [14] P. Zanardi, H. T. Quan, X. Wang, and C. P. Sun, Mixed-state fidelity and quantum criticality at finite temperature, *Phys. Rev. A* **75**, 032109 (2007).
- [15] M. Cozzini, P. Giorda, and P. Zanardi, Quantum phase transitions and quantum fidelity in free fermion graphs, *Phys. Rev. B* **75**, 014439 (2007).
- [16] M. Heyl, A. Polkovnikov, and S. Kehrein, Dynamical quantum phase transitions in the transverse-field ising model, *Phys. Rev. Lett.* **110**, 135704 (2013).
- [17] N. O. Abeling and S. Kehrein, Quantum quench dynamics in the transverse field ising model at nonzero temperatures, *Phys. Rev. B* **93**, 104302 (2016).
- [18] R. Jafari and H. Johannesson, Loschmidt echo revivals: Critical and noncritical, *Phys. Rev. Lett.* **118**, 015701 (2017).
- [19] B. Mera, C. Vlachou, N. Paunković, V. R. Vieira, and O. Viyuela, Dynamical phase transitions at finite temperature from fidelity and interferometric loschmidt echo induced metrics, *Phys. Rev. B* **97**, 094110 (2018).
- [20] A. Mostafazadeh, Pseudo-hermiticity versus pt symmetry: the necessary condition for the reality of the spectrum of a non-hermitian hamiltonian, *J. Math. Phys.* **43**, 205 (2002).
- [21] C. M. Bender, D. C. Brody, and H. F. Jones, Complex extension of quantum mechanics, *Phys. Rev. Lett.* **89**, 270401 (2002).
- [22] C. M. Bender and S. Boettcher, Real spectra in non-hermitian hamiltonians having pt symmetry, *Phys. Rev. Lett.* **80**, 5243 (1998).
- [23] C. M. Bender, S. Boettcher, and P. N. Meisinger, Pt-symmetric quantum mechanics, *J. Math. Phys.* **40**, 2201 (1999).
- [24] A. Mostafazadeh, Spectral singularities of complex scattering potentials and infinite reflection and transmission coefficients at real energies, *Phys. Rev. Lett.* **102**, 220402 (2009).
- [25] S. Longhi, Exceptional points and bloch oscillations in non-hermitian lattices with unidirectional hopping, *EPL (Europhysics Letters)* **106**, 34001 (2014).
- [26] L. Jin and Z. Song, Incident direction independent wave propagation and unidirectional lasing, *Phys. Rev. Lett.* **121**, 073901 (2018).
- [27] X. Z. Zhang, L. Jin, and Z. Song, Dynamic magnetization in non-hermitian quantum spin systems, *Phys. Rev. B* **101**, 224301 (2020).
- [28] J. Dalibard, Y. Castin, and K. Mølmer, Wave-function approach to dissipative processes in quantum optics, *Phys. Rev. Lett.* **68**, 580 (1992).
- [29] R. Dum, P. Zoller, and H. Ritsch, Monte carlo simulation of the atomic master equation for spontaneous emission, *Phys. Rev. A* **45**, 4879 (1992).
- [30] K. Mølmer, Y. Castin, and J. Dalibard, Monte carlo wave-function method in quantum optics, *J. Opt. Soc. Am. B* **10**, 524 (1993).
- [31] H. M. Wiseman, Quantum trajectories and quantum measurement theory, *Quantum Semiclass. Opt.* **8**, 205 (1996).
- [32] M. B. Plenio and P. L. Knight, The quantum-jump approach to dissipative dynamics in quantum optics, *Rev. Mod. Phys.* **70**, 101 (1998).
- [33] T. E. Lee and C.-K. Chan, Heralded magnetism in non-hermitian atomic systems, *Phys. Rev. X* **4**, 041001 (2014).
- [34] S. Sachdev and A. P. Young, Low temperature relax-

- ational dynamics of the ising chain in a transverse field, *Phys. Rev. Lett.* **78**, 2220 (1997).
- [35] See Supplemental Material for the details on derivation of the nonlocal operator D with uniform (Sec. A) as well as disordered (Sec. B) parameters J and g , and in Sec. C approximate calculation of the Loschmidt echo in a larger N , which includes Refs. [4, 8, 36, 44].
- [36] P. Jordan and E. P. Wigner, über das paulische äquivalenzverbot, in *The Collected Works of Eugene Paul Wigner* (Springer, 1993) pp. 109–129.
- [37] D. C. Brody and E.-M. Graefe, Mixed-state evolution in the presence of gain and loss, *Phys. Rev. Lett.* **109**, 230405 (2012).
- [38] K. Kawabata, Y. Ashida, and M. Ueda, Information retrieval and criticality in parity-time-symmetric systems, *Phys. Rev. Lett.* **119**, 190401 (2017).
- [39] A. Uhlmann, The “transition probability” in the state space of a *-algebra, *Rep. Math. Phys.* **9**, 273 (1976).
- [40] N. T. Jacobson, L. C. Venuti, and P. Zanardi, Unitary equilibration after a quantum quench of a thermal state, *Phys. Rev. A* **84**, 022115 (2011).
- [41] This is also verified by the approximate calculation of LEs in a larger N (See Sec. C of the Supplemental Material [35]). It indicates that when $g < 1$, the average LEs decays with exponential law close to the boundary (small j). A finite-size scaling based on the approximate calculation is also given..
- [42] P. Huang, X. Kong, N. Zhao, F. Shi, P. Wang, X. Rong, R.-B. Liu, and J. Du, Observation of an anomalous decoherence effect in a quantum bath at room temperature, *Nat. Commun.* **2**, 1 (2011).
- [43] C. M. Sánchez, A. K. Chattah, K. X. Wei, L. Buljubasich, P. Cappellaro, and H. M. Pastawski, Perturbation independent decay of the loschmidt echo in a many-body system, *Phys. Rev. Lett.* **124**, 030601 (2020).
- [44] T. Kimura, Explicit description of the zassenhaus formula, *Prog. Theor. Exp. Phys.* **2017**, 041A03 (2017).

SUPPLEMENTAL MATERIAL

K. L. Zhang and Z. Song*

School of Physics, Nankai University, Tianjin 300071, China

*songtc@nankai.edu.cn

In this Supplemental Material, we present **A.** Derivation of the operator D : uniform case; **B.** Derivation of the operator D : disordered case; and **C.** Approximate calculation of the Loschmidt echo in a larger N .

A. Derivation of the operator D : uniform case

Starting from the Ising chain Hamiltonian H with $J = 1$ in the Letter, one can perform the Jordan-Wigner transformation [36]

$$\begin{aligned}\sigma_j^x &= \prod_{l < j} (1 - 2c_l^\dagger c_l) (c_j + c_j^\dagger), \\ \sigma_j^z &= 2c_j^\dagger c_j - 1,\end{aligned}\tag{S1}$$

to replace the Pauli operators by the fermionic operators c_j . The Hamiltonian is transformed to the Kitaev model [4]

$$H_{\text{Kitaev}} = - \sum_{j=1}^{N-1} (c_j^\dagger c_{j+1} + c_j^\dagger c_{j+1}^\dagger) + \text{H.c.} + g \sum_{j=1}^N (2c_j^\dagger c_j - 1).\tag{S2}$$

To get the solution of the model, we introduce the Majorana fermion operators $a_j = c_j^\dagger + c_j, b_j = -i(c_j^\dagger - c_j)$, which satisfy the commutation relations $\{a_j, a_{j'}\} = 2\delta_{j,j'}, \{b_j, b_{j'}\} = 2\delta_{j,j'}, \{a_j, b_{j'}\} = 0$. Then the Majorana representation of the original Hamiltonian is

$$H_M = -\frac{i}{2} \sum_{j=1}^{N-1} b_j a_{j+1} - \frac{i}{2} g \sum_{j=1}^N a_j b_j + \text{H.c.},\tag{S3}$$

the core matrix of which is that of a $2N$ -site Su-Schrieffer-Heeger (SSH) chain in single-particle invariant subspace. Based on the exact diagonalization result of the SSH chain, the Hamiltonian H_{Kitaev} can be written as the diagonal form

$$H_{\text{Kitaev}} = \sum_{n=1}^N \varepsilon_n \left(d_n^\dagger d_n - \frac{1}{2} \right).\tag{S4}$$

Here d_n is a fermionic operator, satisfying $\{d_n, d_{n'}\} = 0$, and $\{d_n, d_{n'}^\dagger\} = \delta_{n,n'}$. On the other hand, we have the relations

$$[d_n, H_{\text{Kitaev}}] = \varepsilon_n d_n, [d_n^\dagger, H_{\text{Kitaev}}] = -\varepsilon_n d_n^\dagger,\tag{S5}$$

which result in the mapping between the eigenstates of H_{Kitaev} . Direct derivation show that, for an arbitrary eigenstate $|\psi\rangle$ of H_{Kitaev} with eigenenergy E , i.e., $H_{\text{Kitaev}} |\psi\rangle = E |\psi\rangle$, state $d_n |\psi\rangle$ ($d_n^\dagger |\psi\rangle$) is also an eigenstate of H_{Kitaev} with the eigenenergy $E - \varepsilon_n$ ($E + \varepsilon_n$), i.e.,

$$H_{\text{Kitaev}} (d_n |\psi\rangle) = (E - \varepsilon_n) (d_n |\psi\rangle)\tag{S6}$$

and

$$H_{\text{Kitaev}} (d_n^\dagger |\psi\rangle) = (E + \varepsilon_n) (d_n^\dagger |\psi\rangle),\tag{S7}$$

if $d_n |\psi\rangle \neq 0$ ($d_n^\dagger |\psi\rangle \neq 0$).

In large N limit, and within the topologically nontrivial region $|g| < 1$ ($g \neq 0$), the edge modes appear with $\varepsilon_N = 0$ and the edge operator d_N can be expressed as

$$d_N = \frac{1}{2} \sqrt{1-g^2} \sum_{j=1}^N \left[(g^{j-1} + g^{N-j}) c_j^\dagger + (g^{j-1} - g^{N-j}) c_j \right], \quad (\text{S8})$$

i.e., d_N is a linear combination of particle and hole operators of spinless fermions c_j on the edge, and we have $[d_N, H_{\text{Kitaev}}] = \varepsilon_N d_N = 0$. Furthermore, applying the inverse Jordan-Wigner transformation, d_N can be expressed as the combination of spin operators,

$$\begin{aligned} D &= \frac{1}{2} \sqrt{1-g^2} \sum_{j=1}^N \prod_{l < j} (-\sigma_l^z) (g^{j-1} \sigma_j^x - i g^{N-j} \sigma_j^y) \\ &= \frac{1}{2} \sqrt{1-g^2} \sum_{j=1}^N g^{j-1} D_j, \end{aligned} \quad (\text{S9})$$

where $D_j = \prod_{l < j} (-\sigma_l^z) \sigma_j^x - i \prod_{l < N-j+1} (-\sigma_l^z) \sigma_{N-j+1}^y$.

In fact, d_N and D are identical, but only in different representations. Thus, from $[d_N, H_{\text{Kitaev}}] = 0$, we have

$$[D, H] = [D^\dagger, H] = 0, \quad (\text{S10})$$

which lead to the degeneracy of the eigenstates. Here we would like to point out that the spectral degeneracy is dependent on a large N limit. Nevertheless, a sufficiently small g still leads to perfect quasidegeneracy in finite-size systems, since from the exact diagonalization result of a finite-size SSH chain we have $\varepsilon_N \sim g^N$. Furthermore, from the canonical commutation relations $\{d_N, d_N^\dagger\} = 1$ and $\{d_N, d_N\} = 0$, we have

$$\{D, D^\dagger\} = 1, D^2 = (D^\dagger)^2 = 0. \quad (\text{S11})$$

Operators D and D_j ($j \in [1, N]$) are nonlocal combinations of spin operators $\{\sigma_j^x\}$ and $\{\sigma_j^y\}$ for a quantum spin system, and D_1 is the main component of D . Operator $D = \frac{1}{2} \sqrt{1-g^2} \sum_j g^{j-1} D_j$ commutes with the Hamiltonian and acts as a raising (or lowering) operator for two degeneracy eigenstates for $g < 1$. Meanwhile, they are essentially spinless fermion operators for the fermion representation of the quantum spin system.

The mechanism of the nonlocal non-Hermitian perturbation in the Letter is based on an exclusive feature of a non-Hermitian system, which is the existence of exceptional point (EP). Unlike the degeneracy in a Hermitian system, two or more eigenstates coalesce into a single eigenstate. Notably, it supports a special dynamics, which has no counterpart in the Hermitian regime. Such an approach can be applied to other models, which possess degenerate spectrum. In general, such a degeneracy is originated from a symmetry, or a fermionic operator commuting with the Hamiltonian. If such an operator is non-Hermitian, then the Jordan block is formed, which allows the EP dynamics to demonstrate the existence of the degenerate spectrum. Technically speaking, this operator can be solved in the fermionic representation, as the edge operator of the fermionic chain.

B. Derivation of the operator D : disordered case

For the Ising chain with position-dependent random J_j and g_j , i.e., $H = -\sum_{j=1}^{N-1} J_j \sigma_j^x \sigma_{j+1}^x + \sum_{j=1}^N g_j \sigma_j^z$, the operator D still exists. In this case, one can perform the above procedure and solve the Schrödinger equation for the corresponding SSH chain with random hopping in single-particle invariant subspace [8]. We have the following solution:

$$D = \frac{1}{2} \sum_{j=1}^N \prod_{l < j} (-\sigma_l^z) (h_j^+ \sigma_j^x - i h_j^- \sigma_j^y), \quad (\text{S12})$$

where

$$\begin{aligned} h_j^+ &= h_1^+ \prod_{m=1}^{j-1} \frac{g_m}{J_m}, \\ h_j^- &= h_N^- \frac{g_N}{J_j} \prod_{m=j+1}^{N-1} \frac{g_m}{J_m}, \end{aligned} \quad (\text{S13})$$

and h_1^+ (h_N^-) is determined by the normalization condition $\sum_{j=1}^N |h_j^\pm|^2 = 1$. The solution of D is robust against disordered perturbation and the corresponding energies ε_N of the edge modes are still exponentially small in N under the condition of the average value of J_m is stronger than the average value of g_m [8]. Then it can be checked that the commutation relations in Eqs. (S10) and (S11) still hold for the operator D with disordered perturbation in large N limit. This leads to the robust degeneracy of the eigenstates, suggesting that the observed results in the Letter still hold in the presence of disordered parameters J and g in the Hamiltonian, which enhances the prospect of experimental realization.

C. Approximate calculation of the Loschmidt echo in a larger N

In this section, we evaluate the Loschmidt echo (LE) under the post-quench Hamiltonian $\mathcal{H} = H + \kappa D_j$ approximately in the two dimensional subspace of $|\psi_n^+\rangle$ and $|\psi_n^-\rangle$ with the initial state $\rho_n(0) = e^{-\beta E_n^+} |\psi_n^+\rangle \langle \psi_n^+| + e^{-\beta E_n^-} |\psi_n^-\rangle \langle \psi_n^-|$. Instead of the exact calculation of the full Hilbert space in the Letter, this allows us to see the finite-size scaling behavior in a larger N . Here $|\psi_n^+\rangle$ and $|\psi_n^-\rangle$ are the eigenstates discussed in Eq. (5) in the Letter, wherein they are degenerate when $g < 1$ in thermodynamic limit. Now we are considering an arbitrary g in finite N , and the energies for these two eigenstates are different.

In the fermion representation, the operator D_j can be expressed as the linear combination of d_n and d_n^\dagger , that is

$$\begin{aligned} D_j &= \left(c_j^\dagger + c_j \right) + \left(c_{N-j+1}^\dagger - c_{N-j+1} \right) \\ &= \sum_{n=1}^N \left[A_n(j) d_n + B_n(j) d_n^\dagger \right], \end{aligned} \quad (\text{S14})$$

where D_j , c_j and d_n are the operators defined in Sec. A, and the j -dependent coefficients $A_n(j)$, $B_n(j)$ can be obtained numerically. Here we evaluate the time evolution operator $\exp(-i\mathcal{H}t)$. Using the Zassenhaus formula [44], we have

$$\begin{aligned} \exp(-i\mathcal{H}t) &= \exp(-i(H + \kappa D_j)t) \\ &= \exp(-iHt) \exp(-i\kappa D_j t) \exp\left(\kappa \frac{t^2}{2} [H, D_j]\right) \exp\left(i \frac{t^3}{6} (2[\kappa D_j, [H, \kappa D_j]] + [H, [H, \kappa D_j]])\right) \\ &\quad \times \exp\left(-\frac{t^4}{24} ([[[H, \kappa D_j], H], H] + 3[[[H, \kappa D_j], H], \kappa D_j] + 3[[[H, \kappa D_j], \kappa D_j], \kappa D_j])\right) \times \dots, \end{aligned} \quad (\text{S15})$$

which can be simplified through the following process: using Eq. S5. and expand the terms after $\exp(-iHt)$ in Taylor series; The terms with $d_{n \neq N}$ and $d_{n \neq N}^\dagger$ have no contribution to the LE in the subspace we considering, thus they can be ignored. Finally, we obtain the time evolution operator approximately

$$\exp(-i\mathcal{H}t) \approx \exp(-iHt) \left\{ 1 - \kappa \frac{A_N(j)}{-\varepsilon_N} [\exp(-i\varepsilon_N t) - 1] d_N - \kappa \frac{B_N(j)}{\varepsilon_N} [\exp(i\varepsilon_N t) - 1] d_N^\dagger \right\}. \quad (\text{S16})$$

Having this result, it is straight forward to calculate the time evolution of the initial state $\rho_n(0)$, by using $d_N |\psi_n^+\rangle = |\psi_n^-\rangle$, $d_N^\dagger |\psi_n^-\rangle = |\psi_n^+\rangle$, $d_N |\psi_n^-\rangle = d_N^\dagger |\psi_n^+\rangle = 0$, and $\exp(-iHt) |\psi_n^\pm\rangle = \exp(-iE_n^\pm t) |\psi_n^\pm\rangle$. Here we calculate the LE in the subspace of the ground state and the first-excited state, with the initial state $\rho_g(0) = e^{-\beta E_g^+} |\psi_g^+\rangle \langle \psi_g^+| + e^{-\beta E_g^-} |\psi_g^-\rangle \langle \psi_g^-|$. The LE in the subspace of the higher-excited states can be calculated similarly. The numerical calculations of the LE and the average LE follow the definitions in Eqs. (12) and (13), respectively, in the Letter. The numerical results of the average LEs under the post-quench Hamiltonian $\mathcal{H} = H + \kappa D_1$ of different system sizes are presented in Fig. S1.

In Fig. S1(a), we plot the average LEs as functions of parameter g for different N . Correspondingly, the derivative of the average LEs with respect to g are plotted in Fig. S1(b) where we can find the pseudo critical point g_{pc} , defined as the maximum point of $\nabla_g \overline{L}(g)$. We can see that the pseudo critical point is closer to the critical point $g_c = 1$ for a larger N . Figs. S1(c) and (d) are $(g_c - g_{\text{pc}})$ and $\left(\nabla_g \overline{L}(g)\right)_{g=g_{\text{pc}}}$ as a function of N in logarithmic scales. We can see that the scaling behaviors are consistent to our expectation: when N becomes larger, the pseudo critical point approaches to 1, and the derivative of the average LEs at the pseudo critical point tends to infinite.

The numerical results of the j -dependent average LEs of initial state $\rho_g(0)$ under the post-quench Hamiltonian $\mathcal{H} = H + \kappa D_j$ are presented in Fig. S2. It indicates that when $g < 1$, the average LEs decay with exponential

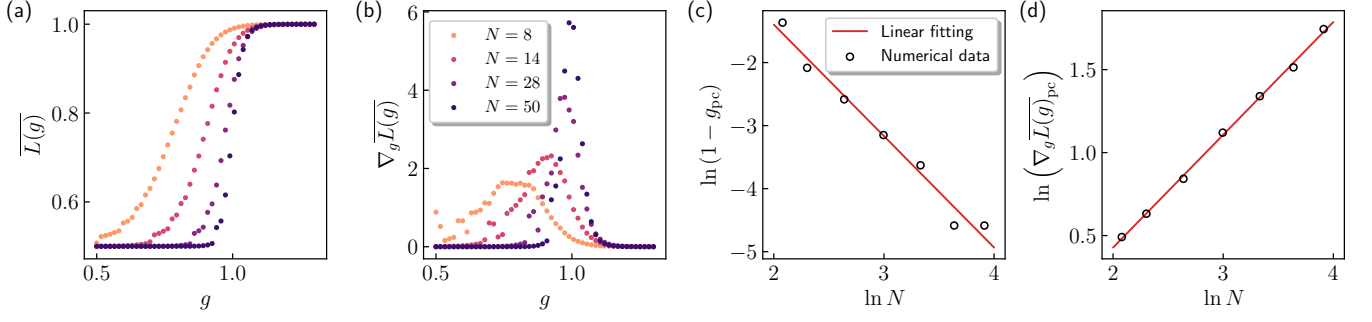


FIG. S1. The numerical results of the average LEs and the finite-size scaling analysis when $j = 1$. (a) and (b) are the average LEs and the derivatives as functions of g for $N = 8, 14, 28$ and 50 . (c) and (d) are $(g_c - g_{pc})$ and $\left(\nabla_g \overline{L}(g)\right)_{g=g_{pc}}$ as a function of N in logarithmic scales, where system sizes $N = 8, 10, 14, 20, 28, 38, 50$ are taken in the numerical calculation, and the numerical data are fitted linearly by $\ln(1 - g_{pc}) = -1.77 \ln N + 2.14$ and $\ln\left(\nabla_g \overline{L}(g)\right)_{g=g_{pc}} = 0.68 \ln N - 0.93$. Other parameters for the numerical calculations are $\tau = 1000$, $T = 2000$, $J = 1$, $\kappa = 0.1$, and $\beta = 10$.

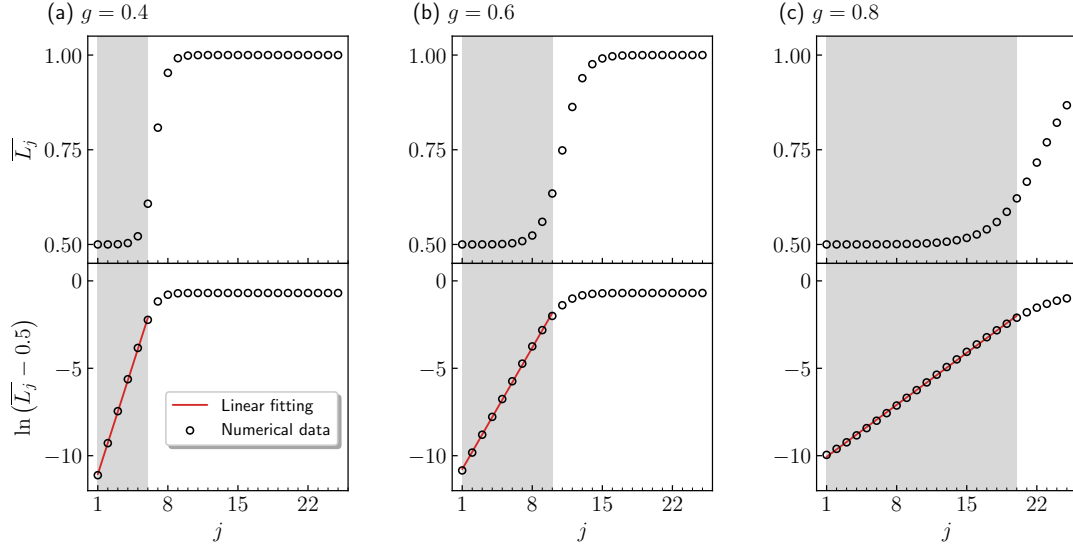


FIG. S2. The numerical results of the average LEs \overline{L}_j as functions of j , for different g : (a) $g = 0.4$; (b) $g = 0.6$ and (c) $g = 0.8$. In the bottom panels, $\ln(\overline{L}_j - 0.5)$ as functions of j are plotted corresponding to the upper panels. The red lines are the linear fittings for the data points in the shaded regions. Other parameters for the numerical calculations are $N = 50$, $\tau = 1000$, $T = 2000$, $J = 1$, $\kappa = 0.1$, and $\beta = 10$.

law $\overline{L}_j = C_1 \exp(C_2 j) + 0.5$ close to the boundary (small j), where C_1 and C_2 are g -dependent real numbers. This suggests the bulk-boundary correspondence at nonzero temperatures in a larger N .